Kuwait J. Sci. Eng. **31**(1) pp. 193-218, 2004

Global bifurcation analysis of two-phase systems in continuous stirred tank reactors

MOHAMED E. E. ABASHAR

Department of Chemical Engineering, College of Engineering, King Saud University, P.O. Box 800, Riyadh 11421, Saudi Arabia. Fax: + 966-1-4678770, E-mail: mabashar@ksu.edu.sa

ABSTRACT

The problem of two-phase stirred tank reactors is considered from the standpoint of global steady state bifurcation analysis. The investigation is based on the singularity theory and dividing the global parameter space into regions with different numbers of solutions and bifurcation diagrams. This approach is shown to be powerful giving new insights, which are so difficult to obtain by numerical and parametric studies. The investigation has uncovered a good part of the multiplicity characteristics in feasible regions of these complicated systems. The problem presents some interesting features of the existence of two singular points of highest codimension (butterfly) in feasible regions. It has been shown that regions of up to five steady states exist and bifurcation diagrams of discontinuous branches are presented.

Keywords: Bifurcation; CSTR ; multi-phase systems, steady-state multiplicity.

INTRODUCTION

Industrially important reactions are mainly heterogeneous systems (Doraiswamy & Sharma, 1984). Large classes of these reactions such as nitrations, sulphonations and alkylations are carried out in two fluid phases. Continuous stirred tank reactors are widely used in these operations. This makes the rational design of the continuous stirred tank reactors in which heterogeneous reactions are carried out a problem of primary interest to the chemical engineer.

The literature on the dynamic behavior of the continuous stirred tank reactors of homogeneous systems is very extensive (Uppal *et al.* 1974, Kubicek & Marek 1983, Kevrekidis *et al.* 1986, Planeaux & Jensen 1986, Abashar & Judd 1998) except for multi-phase systems (Pais & Portugal 1996). This could be due to the fact that in multi-phase systems the hydrodynamic is very complex as well as the interaction of mass and heat transport and chemical reactions (Elnashaie & Abashar 1994, Abashar & Elnashaie 1997, Abashar *et al.* 1997, Gladden *et al.* 2002). In comprehensive articles, Schmitz & Amundson (1963a,b) created

models which simulate the physical rate processes of heat and mass transfer between phases of perfectly mixed two-phase systems. The authors, inspired by the graphical work of Van Heerden (1953) used the models to analyze the multiplicity and stability of steady state solutions of perfectly mixed two-phase systems in physical equilibrium. Only three steady states at certain parameters were presented. The stability criteria were obtained by linearization.

Chemical engineers have become very interested in studying the global multiplicity features of chemical systems in multi-parameter space using the singularity theory (Golubitsky & Schaeffer 1979, 1985, Gilmore 1981, Balakotaiah & Luss 1981, 1982, 1984). The singularity theory has been shown to be a powerful mathematical technique for the analysis of steady state solutions of lumped-parameter systems.

In the present paper, the singularity theory is implemented for treating the problem of a highly non-linear two-phase system in physical equilibrium. The technique used here appears to be more powerful than the previous techniques (graphical and numerical studies) and opens the possibility for significant new results.

MATHEMATICAL FORMULATION OF THE PROBLEM

The problem investigated is that of a single, first order, exothermic reaction

$$A \rightarrow R$$

taking place in a CSTR into which liquid phases α and β are fed continuously. The specific reaction rate constants in phase α and β are given by:

$$k^{\alpha}(T) = k_o^{\alpha}\, e^{-E^{\alpha}/RT} \tag{1}$$

$$k^{\beta}(T) = k_o^{\beta}\, e^{-E^{\beta}/RT} \tag{2}$$

A schematic diagram of the reactor is shown in Fig. 1. The following simplifying assumptions are used in the derivation of the conservation equations of the model:

1 - The reactor operates at steady state conditions.

2 - The system is a dilute liquid-liquid system and the phases are completely immiscible liquids.

3 - The system is perfectly mixed i.e. no distributions of any kind within the system.

4 - Interfacial transfer rates are rapid and the system is in physical equilibrium.

5 - The temperature of the phases is equal.

6 - The reaction rate alone is controlling the rate of conversion.

7 - The properties of solvents, α and β are constant with respect to the temperature and concentration.

8 - Heats of solution are neglected.

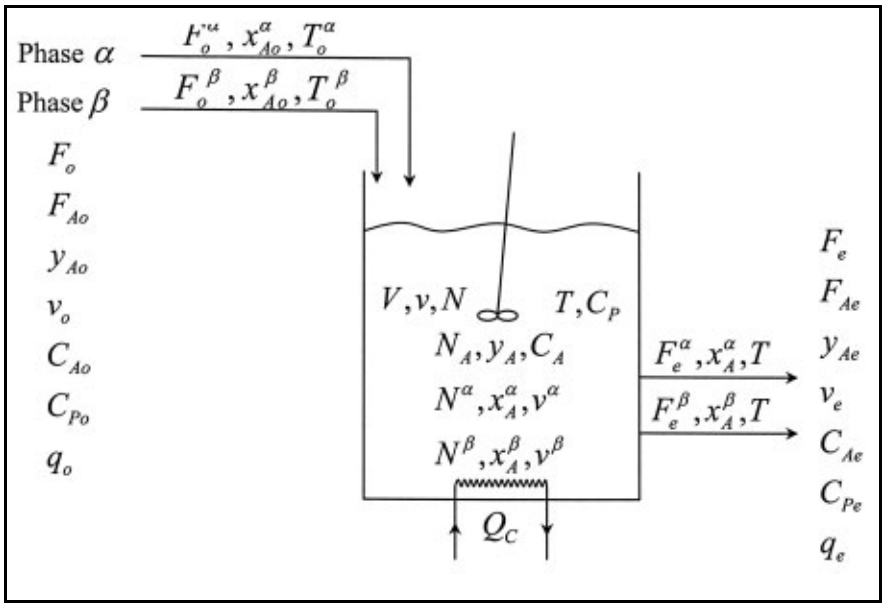

Fig.1. Schematic representation of the continuous stirred tank reactor.

The system is governed by the following mass and energy balance equations:

The steady state mass balance on component A gives

$$\left(F_o^{\alpha} x_{Ao}^{\alpha} + F_o^{\beta} x_{Ao}^{\beta}\right) - \left(F_e^{\alpha} x_A^{\alpha} + F_e^{\beta} x_A^{\beta}\right) - \left(k^{\alpha} N^{\alpha} x_A^{\alpha} + k^{\beta} N^{\beta} x_A^{\beta}\right) = 0 \tag{3}$$

and the steady state energy balance gives

$$\begin{aligned}\left(F_o^{\alpha} C_p^{\alpha} T_o^{\alpha} + F_o^{\beta} C_p^{\beta} T_o^{\beta}\right) + (-\Delta H_R)\left(k^{\alpha} N^{\alpha} x_A^{\alpha} + k^{\beta} N^{\beta} x_A^{\beta}\right) \\ - \left(F_e^{\alpha} C_p^{\alpha} + F_e^{\beta} C_p^{\beta}\right) T - U(T - T_C) = 0.\end{aligned} \tag{4}$$

The two phases are in physical equilibrium and the components are distributed between the phases according to the following equilibrium relationship

$$x_A^{\beta} = K_A x_A^{\alpha}. \tag{5}$$

The holding time for each phase is defined by

$$\tau^{\alpha} = \frac{N^{\alpha}}{F_o^{\alpha}}, \quad \tau^{\beta} = \frac{N^{\beta}}{F_o^{\beta}} \tag{6}$$

and the ratio of the holding times is given by

$$\varepsilon = \frac{\tau^{\alpha}}{\tau^{\beta}} \tag{7}$$

and the molar ratio of the phases is defined as

$$\phi = \frac{N^{\beta}}{N^{\alpha}}. \tag{8}$$

Experiments have shown that the ratio of the phases in the reactor is an independent parameter (Trambouze 1961, Schmitz & Amundson 1963a) and may be related to exit flow rates as

$$\frac{F_e^{\beta}}{F_e^{\alpha}} = \varepsilon \frac{N^{\beta}}{N^{\alpha}} = \varepsilon \phi. \tag{9}$$

In two-phase systems, overall quantities inside the reactor are not equal to overall quantities leaving the reactor. The overall mole fraction of component $A(y_A)$, overall molar volume (v), overall concentration of $A(C_A)$ and the overall heat capacity (C_p) within the reactor are given by:

$$y_A = \frac{N_A}{N} = \frac{N^{\alpha} x_A^{\alpha} + N^{\beta} x_A^{\beta}}{(N^{\alpha} + N^{\beta})} = \frac{x_A^{\alpha} + \phi\, x_A^{\beta}}{(1+\phi)} = \frac{x_A^{\alpha}\left(1+\phi\, K_A\right)}{(1+\phi)}, \tag{10}$$

$$v = \frac{V}{N} = \frac{N^{\alpha} v^{\alpha} + N^{\beta} v^{\beta}}{(N^{\alpha} + N^{\beta})} = \frac{v^{\alpha} + \phi\, v^{\beta}}{(1+\phi)}, \tag{11}$$

$$C_A = \frac{N_A}{V} = \frac{N^{\alpha} x_A^{\alpha} + N^{\beta} x_A^{\beta}}{V} = \frac{x_A^{\alpha}\left(1+\phi\, K_A\right)}{v^{\alpha} + \phi\, v^{\beta}} = \frac{y_A}{v}, \text{ and} \tag{12}$$

$$C_P = \frac{N^{\alpha} C_P^{\alpha} + N^{\beta} C_P^{\beta}}{(N^{\alpha} + N^{\beta})} = \frac{C_P^{\alpha} + \phi\, C_P^{\beta}}{(1+\phi)}. \tag{13}$$

Similarly at the exit of the reactor:

$$y_{Ae} = \frac{F_{Ae}}{F_e} = \frac{F_e^{\alpha} x_A^{\alpha} + F_e^{\beta} x_A^{\beta}}{(F_e^{\alpha} + F_e^{\beta})} = \frac{x_A^{\alpha} + \varepsilon\,\phi\, x_A^{\beta}}{(1+\varepsilon\,\phi)} = \frac{x_A^{\alpha}\left(1+\varepsilon\,\phi\, K_A\right)}{(1+\varepsilon\phi)}, \tag{14}$$

$$v_e = \frac{q_e}{F_e} = \frac{F_e^{\alpha} v^{\alpha} + F_e^{\beta} v^{\beta}}{(F_e^{\alpha} + F_e^{\beta})} = \frac{v^{\alpha} + \varepsilon\,\phi\, v^{\beta}}{(1+\varepsilon\,\phi)}, \tag{15}$$

$$C_{Ae} = \frac{F_{Ae}}{q_e} = \frac{F_e^{\alpha} x_A^{\alpha} + F_e^{\beta} x_A^{\beta}}{F_e^{\alpha} v^{\alpha} + F_e^{\beta} v^{\beta}} = \frac{x_A^{\alpha}\left(1+\varepsilon\,\phi\, K_A\right)}{v^{\alpha} + \varepsilon\,\phi\, v^{\beta}} = \frac{y_{Ae}}{v_e}, \text{ and} \tag{16}$$

$$C_{Pe} = \frac{F_e^{\alpha} C_P^{\alpha} + F_e^{\beta} C_P^{\beta}}{(F_e^{\alpha} + F_e^{\beta})} = \frac{C_P^{\alpha} + \varepsilon\ \phi\ C_P^{\beta}}{(1+\varepsilon\,\phi)}. \tag{17}$$

Let the symbol r will be used to designate the ratio of an overall quantity in the exit stream to that inside the reactor, then:

$$r_y = \frac{y_{Ae}}{y_A} == \frac{(1+\varepsilon\,\phi\ K_A)(1+\phi)}{(1+\phi\, K_A)(1+\varepsilon\phi)}, \tag{18}$$

$$r_v = \frac{v_e}{v} = \frac{(1+\varepsilon\,\phi\ v^{\beta}/v^{\alpha})(1+\phi)}{(1+\phi\ v^{\beta}/v^{\alpha})(1+\varepsilon\phi)}, \text{ and} \tag{19}$$

$$r_{C_P} = \frac{C_{pe}}{C_p} = \frac{(1+\varepsilon\,\phi\, C_P^{\beta}/C_P^{\alpha})(1+\phi)}{(1+\phi\, C_P^{\beta}/C_P^{\alpha})(1+\varepsilon\phi)}. \tag{20}$$

Let y^{α} and y_e^{α} will be used as the mole fractions of solvent α inside the reactor and in the exit stream respectively. Then,

$$y^{\alpha} = \frac{N^{\alpha}}{N} = \frac{N^{\alpha}}{N^{\alpha} + N^{\beta}} = \frac{1}{(1+\phi)}, \tag{21}$$

$$y_e^{\alpha} = \frac{F_e^{\alpha}}{F_e} = \frac{F_e^{\alpha}}{F_e^{\alpha} + F_e^{\beta}} = \frac{1}{(1+\varepsilon\,\phi)}, \tag{22}$$

$$r_{\alpha} = \frac{y_e^{\alpha}}{y^{\alpha}} = \frac{(1+\phi)}{(1+\varepsilon\,\phi)}. \tag{23}$$

If the densities of the phases are constant, the volumetric flow rates at the inlet (q_o) and exit (q_e) of the reactor should be the same. Thus,

$$F_o v_o = F_e v_e = F_e \nu r_v \tag{24}$$

and the total holding time is given by

$$\tau = \frac{V}{q_o} = \frac{V}{F_o v_o} = \frac{N}{F_e r_v} = \left(\frac{r_\alpha}{r_v}\right)\tau^\alpha = \left(\frac{r_\beta}{r_v}\right)\tau^\beta. \tag{25}$$

Let the ratio of volumetric heat capacity of reactor contents to volumetric heat capacity of the feed is given by:

$$\psi = \frac{\left(C_P / \nu\right)}{\left(C_{Po} / v_o\right)}. \tag{26}$$

Substitution of the above definition into the mass and energy balance equations (Eqs. 3 and 4) gives:

$$1 - \left[\frac{r_v}{r_v}\right]\left[\frac{C_A}{C_{Ao}}\right] - \frac{\tau\left[k_o^\alpha e^{-E^\alpha/RT} + k_o^\beta e^{-E^\beta/RT}\phi K_A\right]}{\left(1+\phi K_A\right)}\left[\frac{C_A}{C_{Ao}}\right] = 0 \quad \text{and} \tag{27}$$

$$T_o + \left[\frac{(-\Delta H_R) y_{Ao}}{C_{Po}}\right]\left[\frac{\tau\left(k_o^\alpha e^{-E^\alpha/RT} + k_o^\beta e^{-E^\beta/RT}\phi K_A\right)}{\left(1+\phi K_A\right)}\right]\left[\frac{C_A}{C_{Ao}}\right] - \left[\frac{r_c}{r_v}\right]\psi T - \frac{U}{F_o C_{po}}\left(T - T_c\right) = 0 \tag{28}$$

where

$$T_o = \frac{T_o^\alpha + \varepsilon\phi\left(C_p^\beta / C_P^\alpha\right)T_o^\beta}{1 + \varepsilon\phi\left(C_p^\beta / C_P^\alpha\right)}. \tag{29}$$

The molar ratio of the phases (ϕ) can be expressed in terms of volume fraction (Ω^α) of phase α as:

$$\phi = \frac{N^{\beta}}{N^{\alpha}} = \frac{V^{\beta}/v^{\beta}}{V^{\alpha}/v^{\alpha}} = \frac{1-\Omega^{\alpha}}{(v^{\beta}/v^{\alpha})\,\Omega^{\alpha}} \tag{30}$$

where

$$\Omega^{\alpha} = \left(\frac{r_v}{r_{\alpha}}\right)\left(\frac{q_o^{\alpha}}{q_o}\right). \tag{31}$$

If the two phases have the same holding time, i.e. $T^{\alpha} = T^{\beta}$, the system will be put into dimensionless form. This may be done by the following substitutions:

$$T^{*} = \frac{T_o + \dfrac{U\,T_c}{F_o\,C_{Po}}}{1+\dfrac{U}{F_o\,C_{Po}}}, \qquad B = \frac{(-\Delta H_R)\,y_{Ao}}{\left[1+\dfrac{U}{F_o\,C_{Po}}\right]C_{Po}T^{*}}, \qquad \gamma^{\alpha} = \frac{E^{\alpha}}{RT^{*}}, \qquad \gamma^{\beta} = \frac{E^{\beta}}{RT^{*}},$$

$$\theta = \frac{\gamma^{\beta}}{\gamma^{\alpha}}, \qquad D_a^{\alpha} = \frac{k^{\alpha}(T^{*})\;\tau\left(1+B\right)}{\left(1+\phi\,K_A\right)}, \qquad D_a^{\beta} = \frac{k^{\beta}(T^{*})\;\tau\phi\;K_A\left(1+B\right)}{\left(1+\phi\,K_A\right)}, \tag{32}$$

$$\lambda = \frac{B\gamma^{\alpha}}{\left(1+B\right)}, \qquad Y = \gamma^{\alpha}\left[1-\frac{T^{*}}{T}\right], \qquad k^{\alpha} = k^{\alpha}(T^{*})\,e^{Y}, \qquad k^{\beta} = k^{\beta}(T^{*})\,e^{\theta Y},$$

and then, equation (27) and (28) may be combined to give a single equation for the dimensionless temperature Y:

$$F(Y,\mathbf{P}) = \left(\lambda\text{-Y}\right)\left[D_a^{\alpha}\,e^{Y} + D_a^{\beta}\,e^{\theta Y}\right] - Y = 0 \tag{33}$$

where the parameter **P** is given as

$$\mathbf{P} = \left(D_a^{\alpha}, D_a^{\beta}, \theta, \lambda\right). \tag{34}$$

The surface described by equation (33) in $(Y,\mathbf{P})$ space is called the steady state manifold. This kind of simplified model may be used to analyze many industrially important chemical reactions such as oximation of cyclohexane and nitration of chlorobenzene.

RESULTS AND DISCUSSION

We are concerned here with how to find feasible regions of parameters in which the maximal number of steady state solutions occur and to determine all possible local bifurcation diagrams. The feasible regions are bounded by:

$$Y_L < Y < Y_U, \text{ and } P_{iL} < P_i < P_{iU}. \tag{35}$$

To accomplish this, the following systematic procedure is considered.

Feasible steady state regions in the global parameter space

In this section we divide the parameter space **P** into feasible steady state regions with different number of solutions. The division is based on the fact that the number of feasible steady state solutions can change only when the **P** space crosses the bifurcation set. The bifurcation set is a singular set on the steady state manifold and satisfies

$$\frac{dF}{dY}(Y, \mathbf{P}) = 0. \tag{36}$$

The procedure is based on finding the singular points of the highest codimension (n). Then, the parameter space in the neighborhood of these singular points is divided into $[(n+3)/2]$ regions. The highest number of solutions is $(n+1)$. The different regions can be found by constructing the locus of all the singular points of codimension $(n+1-2m)$ in the feasible (P_{2m-1}, P_{2m}) space $(m = 1, 2, ..., l)$ for a specific set of the first $(2m-2)$ parameters. The procedure continues until $l = n/2$, when n is even, and $l = (n-1)/2$, when n is odd.

Determination of singular points of the highest codimension

The parameter space **P** (Eq. 34) considered in this investigation has four parameters. Therefore, the codimension of the highest order singularity of Eq. 33 is equal to 4 (butterfly), i.e. the number of parameters that must be adjusted for a given bifurcation to occur generically. To determine the highest order singularity, the set of the equations

$$F = \frac{dF}{dY} = \frac{d^2F}{dY^2} = \frac{d^3F}{dY^3} = \frac{d^4F}{dY^4} = 0 \tag{37}$$

should be solved. By introducing

$$x_1 = D_a^{\alpha}\, e^{Y},$$

$$x_2 = (\lambda - Y) D_a^{\alpha}\, e^{Y},$$

$$x_3 = D_a^{\beta}\, e^{\theta Y}, \tag{38}$$

$$x_4 = (\lambda - Y) D_a^{\beta}\, e^{\theta Y}, \text{ and}$$

$$x_5 = Y$$

the five simultaneous equations (37) can be written as:

$$x_2 + x_4 - x_5 = 0, \tag{39}$$

$$-x_1 + x_2 - x_3 + \theta x_4 - 1 = 0, \tag{40}$$

$$-2x_1 + x_2 - 2\theta x_3 + \theta^2 x_4 = 0, \tag{41}$$

$$-3x_1 + x_2 - 3\theta^2 x_3 + \theta^3 x_4 = 0, \tag{42}$$

$$-4x_1 + x_2 - 4\theta^3 x_3 + \theta^4 x_4 \tag{43}$$

Simple algebraic manipulations give the solution of the equations (39-43) as follows

$$x_1 = \frac{\theta^2}{(\theta-1)^2},\ x_2 = \frac{2(\theta-2)\theta^2}{(\theta-1)^3},\ x_3 = \frac{1}{(\theta-1)^2},\ x_4 = \frac{2(2\theta-1)}{\theta(\theta-1)^3},$$
$$\text{and } x_5 = \frac{2(1+\theta)}{\theta}. \tag{44}$$

Substitution of these values into equation (38) gives:

$$
\begin{aligned}
Y &= \frac{2(1+\theta)}{\theta}, \\
D_a^{\alpha} &= \frac{\theta^2}{(\theta-1)^2} e^{-\frac{2(1+\theta)}{\theta}}, \\
D_a^{\beta} &= \frac{1}{(\theta-1)^2} e^{-2(1+\theta)}, \text{ and} \\
\lambda &= 4 + \frac{2}{\theta(1-\theta)}.
\end{aligned}
\tag{45}
$$

From equation (38), we have $\frac{x_1}{x_3} = \frac{x_2}{x_4}$. (46)

It follows from equation (46) that $\theta^2 - 4\theta + 1 = 0$ (47)

The solution of this quadratic equation gives $\theta = 2 \pm \sqrt{3}$ (48)

In this case we have two positive roots i.e. two singular points (butterfly) of codimension four in the $(Y, D_a^{\alpha}, D_a^{\beta}, \theta, \lambda)$

$$\frac{d^5 F}{dY^5} = -\theta^2 \neq 0. \tag{49}$$

The coordinates of butterfly point 1 $(\theta = 2 + \sqrt{3})$ and butterfly point 2$(\theta = 2 - \sqrt{3})$ are (2.53590, 0.147772, 0.103948×10^{-4}, 3.73205, 3.80385) and (9.46410, 0.103948×10^{-4}, 0.147772, 0.26795, 14.19615), respectively.

Locus of swallowtail points

To divide the parameter space **P** into regions of different number of solutions, we construct the loci of the singular points of codimension three (swallowtail points) emanating from each butterfly point. The loci are defined by

$$\frac{d^i F}{dY^i} = 0, \qquad i = 0, 1, 2, 3 \tag{50}$$

and

$$\frac{d^4 F}{dY^4} \neq 0. \tag{51}$$

By introducing

$$\begin{aligned} x_1 &= D_a^{\alpha}\, e^{Y}, \\ x_2 &= D_a^{\beta}\, e^{\theta Y}, \\ x_3 &= \lambda - Y, \end{aligned} \tag{52}$$

and simple algebraic manipulations, the four simultaneous equations (50) give

$$2\theta\left(\theta^2 - 6\theta + 1\right)\lambda^2 - 8(1+\theta)(\theta^2 - 7\theta + 1)\lambda - 216\theta = 0. \tag{53}$$

Figure 2 shows the locus of swallowtail points (codimension 3) emanating from the butterfly point 1 in the (θ, λ) plane. The locus forms a cusp, which divides the plane into two regions 1 and 2. Equation (33) has a maximum of five solutions for some $(D_a^{\alpha}, D_a^{\beta})$ if and only if (θ, λ) inside region 1. For (θ, λ) inside region 2, equation (33) has a maximum of three solutions for some $(D_a^{\alpha}, D_a^{\beta})$.

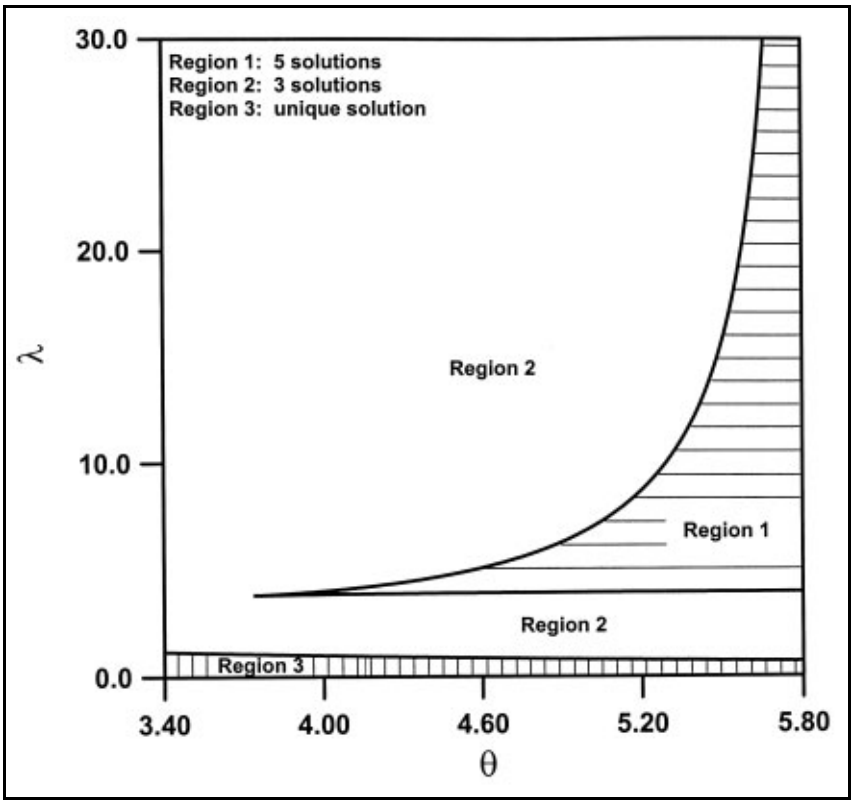

Fig.2. Locus of the swallowtail points in the (θ, λ) plane for the butterfly singularity 1 ($Y = 2.53590,\ D_a^{\alpha} = 0.147772,\ D_a^{\beta} = 0.103948 \times 10^{-4},\ \theta = 3.73205,\ \lambda = 3.80385$).

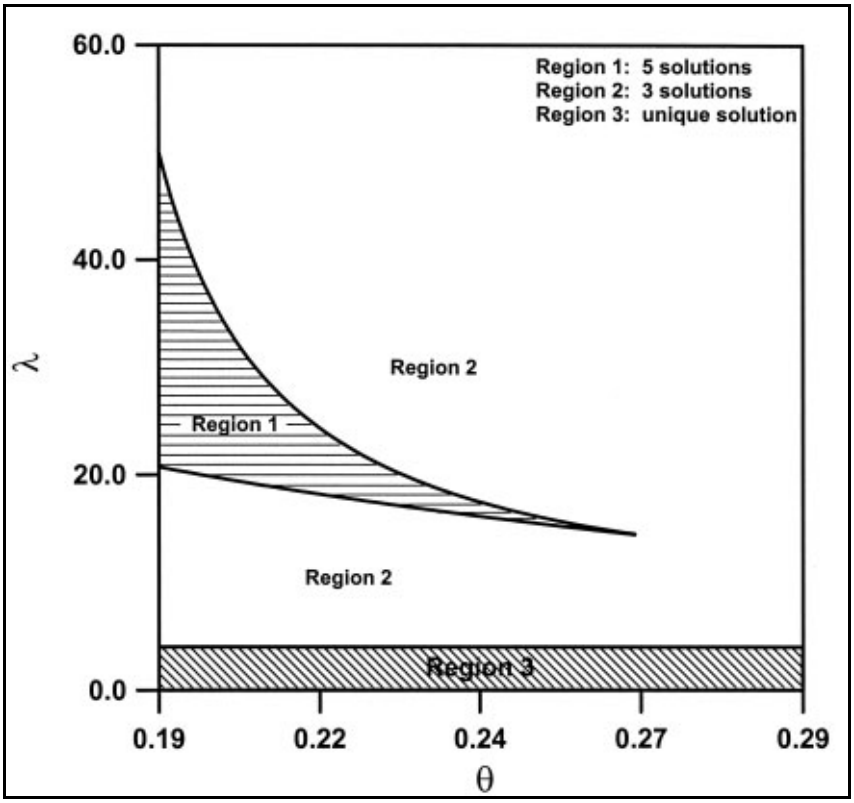

Fig.3. Locus of the swallowtail point in the (θ, λ) plane for the butterfly singularity 2 ($Y = 9.46410,\ D_a^{\alpha} = 0.103948 \times 10^{-4},\ D_a^{\beta} = 0.0.147772,\ \theta = 0.26795,\ \lambda = 14.19615$).

Similarly the locus of swallowtail points emanating from the butterfly point 2 in the (θ, λ) plane is shown in Fig. 3. Region 1 of the unique solution shown in Figs. 2 and 3 is constructed from the analysis of the fold points (codimension 1) presented in the next section.

Locus of fold points

The locus of the fold points (singular points of codimension 1) is given by

$$F = \frac{dF}{dY} = 0 \tag{54}$$

and

$$\frac{d^2F}{dY^2} \neq 0. \tag{55}$$

By simple algebraic manipulations, the two simultaneous equations (54) give

$$D_a^{\alpha} = \frac{\left(\theta Y^2 - \theta\lambda Y + \lambda\right)e^{-Y}}{(1-\theta)(\lambda - Y)^2} \tag{56}$$

and

$$D_a^{\beta} = \frac{\left(Y^2 - \lambda Y + Y\right)e^{-\theta Y}}{(\theta - 1)(\lambda - Y)^2}. \tag{57}$$

For $\theta > 1$ and $\lambda < \dfrac{4}{\theta}$, D_a^{α} is negative and the fold points cannot exist in the feasible region. Therefore, a unique solution for all $(D_a^{\alpha}, D_a^{\beta})$ exists as shown by Regions 1 in Fig. 2. For $0 < \theta < 1$ and $\lambda < 4$, D_a^{β} is negative and the fold points cannot exist in the feasible region. Thus, a unique solution for all $(D_a^{\alpha}, D_a^{\beta})$ exists as shown by Region 1 in Fig. 3.

In the analyses that follow, we consider the butterfly singular point 2. We construct the loci of the fold points for two points in region 1 and 2 shown in Fig. 3. Point 1 at $(\theta = 0.19,\ \lambda = 21.0)$ inside region 1 and point 2 at $(\theta = 0.20, \lambda = 8.0)$ inside region 2. For point 1 $(\theta = 0.19,\ \lambda = 21.0)$ the locus of the fold points is shown in Fig. 4. It is clear that the locus of the fold points divides the $(D_a^{\alpha}, D_a^{\beta})$ plane into three regions of 1,3 and 5 solutions as shown in Fig. 4 (a) and the enlargement part of Fig. 4 (a) that is shown in Fig. 4 (b).

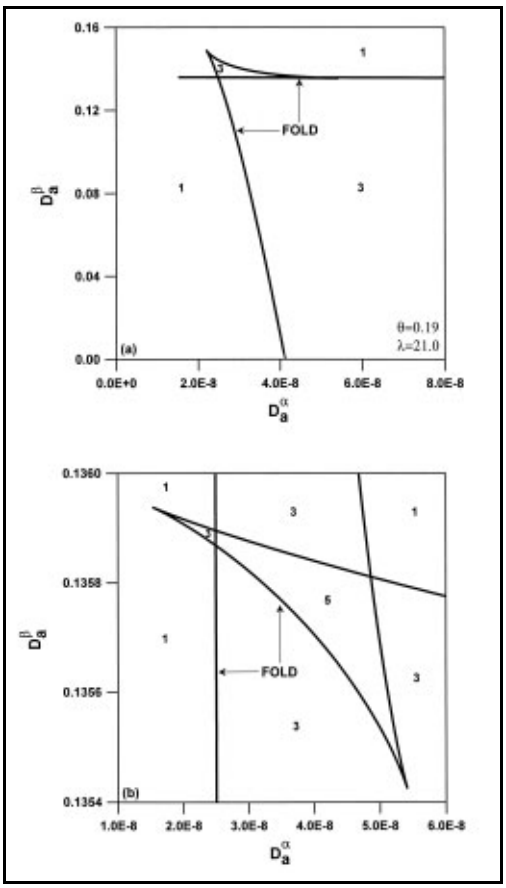

Fig.4. Locus of the fold points in the $(D_a^{\alpha}, D_a^{\beta})$ plane for the point $(\theta = 0.19,\ \lambda = 21.0)$ in region 1 shown in Fig.3. (a) Overall diagram; (b) Enlargement of the part of the locus.

Determination of the multiplicity patterns

The next step is to determine all the possible types of bifurcation diagrams for the regions shown in Fig. 4, i.e. the dependence of the steady state solutions of Eqn. 33 on the values of the parameter **P**. It is known from the singularity theory that three varieties of bifurcation surfaces and special parameter sets can affect the qualitative features of a bifurcation diagram. The bifurcation surfaces are: the hysteresis variety (H), the isola variety (I) and the double-limit variety (DL). The special parameter sets are: the boundary limit set (BLS), the cross limit set (CLS), the double cross set (DCS), the corner set (CS) and the boundary tangent set (BTS) (Balakotaiah & Luss 1984). We consider in this study the bifurcation surfaces and the boundary limit set (BLS) which is the most commun one.

Let us assume that Eqn. 33 can be written as

$$F(Y, D_a^{\beta}, \mathbf{P}^*) = 0 \tag{58}$$

where D_a^{β} is a bifurcation parameter and $\mathbf{P}^*$ is a vector of parameters, defined by

$$\mathbf{P}^* = (D_a^{\alpha}, \theta, \lambda). \tag{59}$$

The features of a bifurcation diagram of 58 may change when the parameters $\mathbf{P}^*$ cross the three bifurcation surfaces and the special limit sets.

Determination of the hysteresis variety (H)

The hysteresis variety (H) defines a feasible surface in the parameter space $\mathbf{P}^*$, which satisfies the following equations

$$F(Y, D_a^{\beta}, \mathbf{P}^*) = \frac{\partial F}{\partial Y}(Y, D_a^{\beta}, \mathbf{P}^*) = \frac{\partial^2 F}{\partial Y^2}(Y, D_a^{\beta}, \mathbf{P}^*) = 0. \tag{60}$$

A simultaneous solution of Eqn. 60 gives

$$\theta Y_H^3 - 2\theta\lambda Y_H^2 + \lambda\left[(\lambda+1)\theta + 1\right]Y_H + \lambda\left[2 - \lambda(1+\theta)\right] = 0 \tag{61}$$

and

$$D_a^{\alpha} = \frac{\left[(\lambda - Y_H)(1 - \theta Y_H) + Y_H\right]e^{-Y_H}}{(1-\theta)(Y_H - \lambda)^2}. \tag{62}$$

Determination of the isola variety (I)

The isola variety defines a feasible surface in the parameter space $\mathbf{P}^*$ which satisfies the following equations:

$$F(Y, D_a^\beta, \mathbf{P}^*) = \frac{\partial F}{\partial Y}(Y, D_a^\beta, \mathbf{P}^*) = \frac{\partial F}{\partial D_a^\beta}(Y, D_a^\beta, \mathbf{P}^*) = 0. \tag{63}$$

A simultaneous solution of equation (63) gives

$$D_a^\alpha + D_a^\beta = -1. \tag{64}$$

Since D_a^α and D_a^β cannot be negative within the feasible region i.e. the isola variety cannot exist in this case.

Determination of the double-limit variety (DL)

The double-limit variety defines a feasible surface in the parameter space $\mathbf{P}^*$ which satisfies the following four equations:

$$\begin{aligned} &F(Y_1, D_a^\beta, \mathbf{P}^*) = F(Y_2, D_a^\beta, \mathbf{P}^*) = 0, \qquad Y_1 \neq Y_2, \text{ and} \\ &\frac{\partial F}{\partial Y}(Y_1, D_a^\beta, \mathbf{P}^*) = \frac{\partial F}{\partial Y}(Y_2, D_a^\beta, \mathbf{P}^*) = 0. \end{aligned} \tag{65}$$

In this case a limit point exists at the feasible boundary.

Determination of the boundary limit set (BLS)

The existence of the boundary limit set may change the features of the bifurcation diagram in the feasible region. The boundary limit set is the set of parameters which satisfies:

$$F(Y, D_a^\beta, \mathbf{P}^*) = \frac{\partial F}{\partial Y}(Y, D_a^\beta, \mathbf{P}^*) = 0 \tag{66}$$

and either

$$Y = Y_{(boundary)} \; or \quad D_a^\beta = D_{a(boundary)}^\beta.$$

At the lower bound of the feasible region i.e. $D_a^\beta = 0$, Eqn. 66 gives

$$Y_{DL}^2 - \lambda Y_{DL} + \lambda = 0. \tag{67}$$

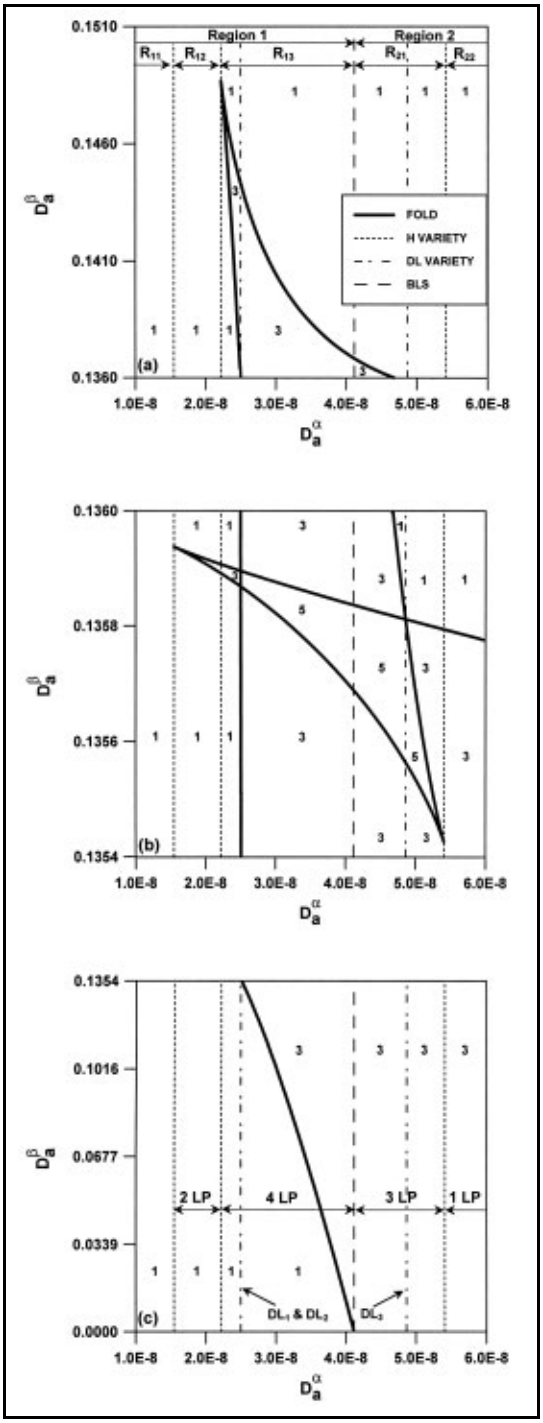

Fig.5. Enlargements of the main part of the locus of the fold points shown in Fig. 4(a) with the hysteresis variety, the double-limit variety and the boundary limit set.

For point 1 at ($\theta = 0.19,\ \lambda = 21.0$) in region 1 (Fig. 3), the hysteresis variety is found at ($D_a^\alpha = 1.546 \times 10^{-8},\ D_a^\alpha = 2.219 \times 10^{-8},\ D_a^\alpha = 5.409 \times 10^{-8}$), the double-limit variety DL_1, DL_2 and DL_3) at ($D_a^\alpha = 2.4991 \times 10^{-8}$, $D_a^\alpha = 2.49958 \times 10^{-8},\ D_a^\alpha = 4.865 \times 10^{-8}$), and the boundary limit at $D_a^\alpha = 4.116965013 \times 10^{-8}$ as shown in Fig.5. The main part of the locus of the fold points shown in Fig. 4(a) is enlarged in Figs. 5 (a), (b) and (c). The bifurcation surfaces and the boundary limit set (BLS) divide the parametric plane (D_a^α, D_a^β) into different regions having different multiplicity patterns.

The boundary limit set (BLS) separates the (D_a^α, D_a^β) plane into two main regions 1 and 2 as shown in Fig. 5. At the boundary limit set, there are four limit points (4 LP) at the intersections of the fold. Number of solutions of 3,5, 3 and 1 can be observed by changing the bifurcation parameter D_a^β as shown in Fig. 6. It is clearly shown that one of the limit points exist on the lower bound ($D_a^\beta = 0$), i.e. a clear violation to the function conditions which implies that the solution branches can exist without singularity in the feasible region.

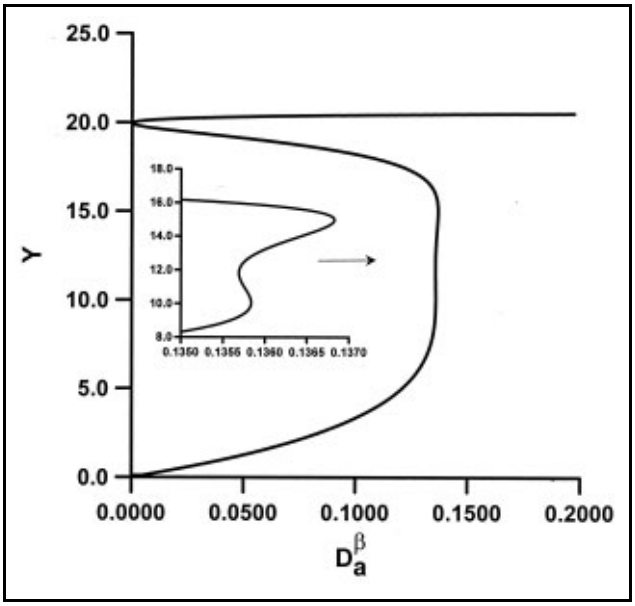

Fig.6. Representative bifurcation diagram at the boundary limit set $D_a^\alpha = 4.116965013 \times 10^{-8}$) shown in Fig.5.

Regions 1 and 2 are subdivided by the hysteresis variety and the double-limit variety (DL) into five subregions, R_{11}, R_{12}, R_{13}, R_{21} and R_{22} according to the number of the limit points (LP) as shown in Fig. 5.

Subregion R_{11}

There is no limit points in this subregion. This is the region of unique solutions for all D_a^α and D_a^β as shown by the representative bifurcation diagram in Fig. 7(a).

Subregion R_{12}

Two limit points (2 LP) exist in this subregion. It is clear that only three steady states are obtained in this subregion as shown in Fig. 5 and by the representative bifurcation diagram in Fig. 7(b).

Subregion R_{13}

This subregion has four limit points (4 LP). The loci of the fold points intersect in this subregion as shown in Fig. 5. Enlargement of this subregion in the neighborhood of the intersections may serve to show the matter more clearly as shown in Fig. 8. Figure 8 shows that the double-limit variety (DL_1, DL_2) passes through these intersections and divides the subregion R_{13} into three regions i, ii and iii. Six bifurcation diagrams can exist in this subregion as shown in Fig. 9. The sequence of the number of solutions in regions i, ii and iii are (1,3,1,3,1), (1,3,5,3,1) and (1,3,5,3,1) respectively as shown in Figs. 5 and 8 and by the representative bifurcation diagrams in Figs. 9 (a), (c) and (e). At the double limit variety (DL_1, DL_2), two limit points coincide as shown in Fig. 9 (b) and (d). This is implies that when $\mathbf{P}^*$ crosses the bouble-limit variety the relative position of the limit points changes.

Subregion R_{21}

Subregion R_{21} contains three limit points (3 LP) as shown in Fig. 10(a). Figure 10(b) shows the bifurcation diagram at the boundary limit set, i.e. at the beginning of this subregion. As it can be seen in Figure 10 (a) that the double limit variety (DL_3) divides this subregion into two regions iv and v. Three types of multiplicity patterns can exist in this subregion as shown by the representative bifurcation diagrams in Figs. 10 (c), (d) and (e). At the double limit variety (DL_3), two limit points coincide as shown in Fig. 10 (d).

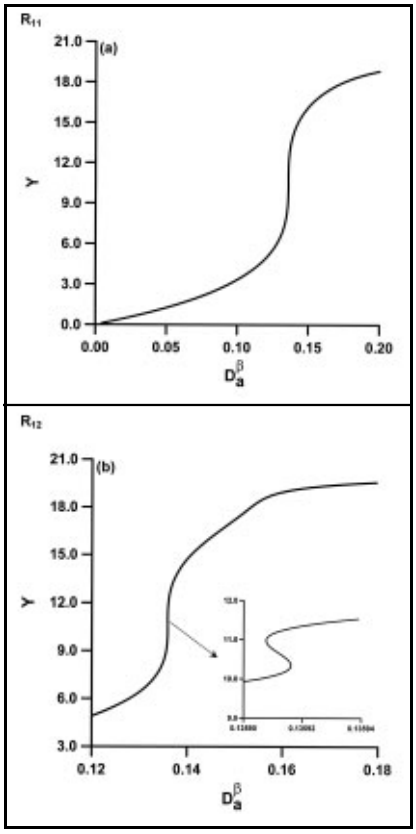

Fig.7. Representative bifurcation diagrams for the subregions R_{11} and R_{12} shown in Fig.5.
(a) Subregion R_{11} ($D_a^{\alpha} = 1.0 \times 10^{-8}$);
(b) Subregion R_{12} ($D_a^{\alpha} = 2.0 \times 10^{-8}$).

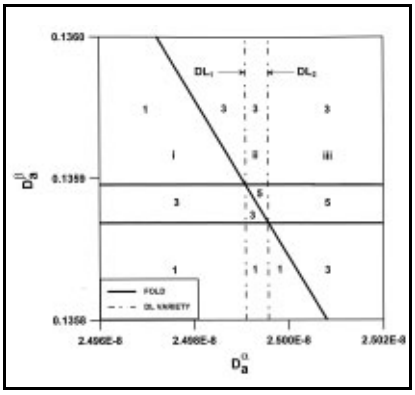

Fig.8. Enlargements of the part of the subregion R_{13} shown in Fig.5.

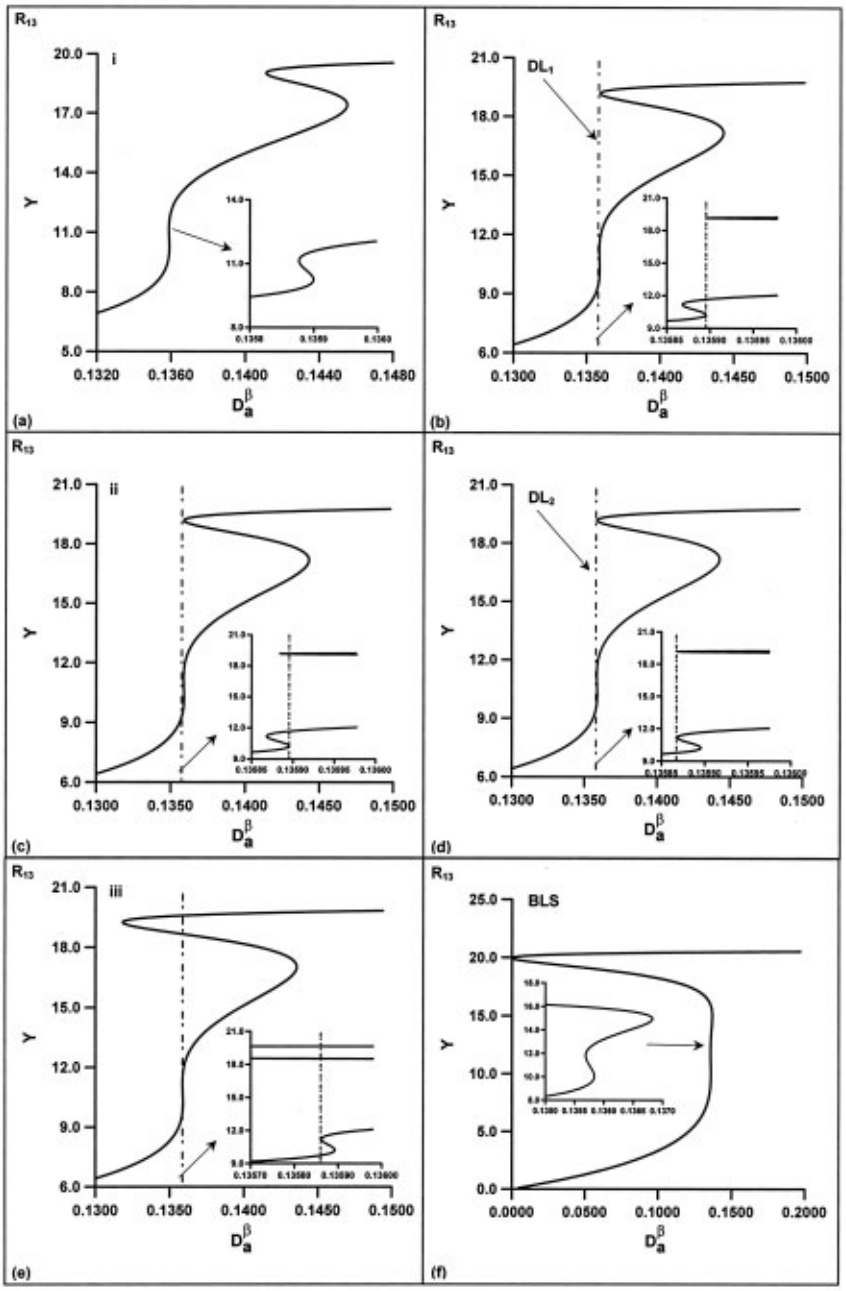

Fig.9. Representative bifurcation diagrams for the subregions R_{13}. (a) Bifurcation diagram at $D_a^{\alpha} = 2.4 \times 10^{-8}$; (b) Bifurcation diagram at the double-limit variety DL_1 ($D_a^{\alpha} = 2.4991 \times 10^{-8}$); (c) Bifurcation diagram at $D_a^{\alpha} = 2.4993 \times 10^{-8}$; (d) Bifurcation diagram at the double-limit variety DL_2 ($D_a^{\alpha} = 2.49958 \times 10^{-8}$); (e) Bifurcation diagram at $D_a^{\alpha} = 2.57 \times 10^{-8}$; (f) Bifurcation diagram at the boundary limit set ($D_a^{\alpha} = 4.116965013 \times 10^{-8}$).

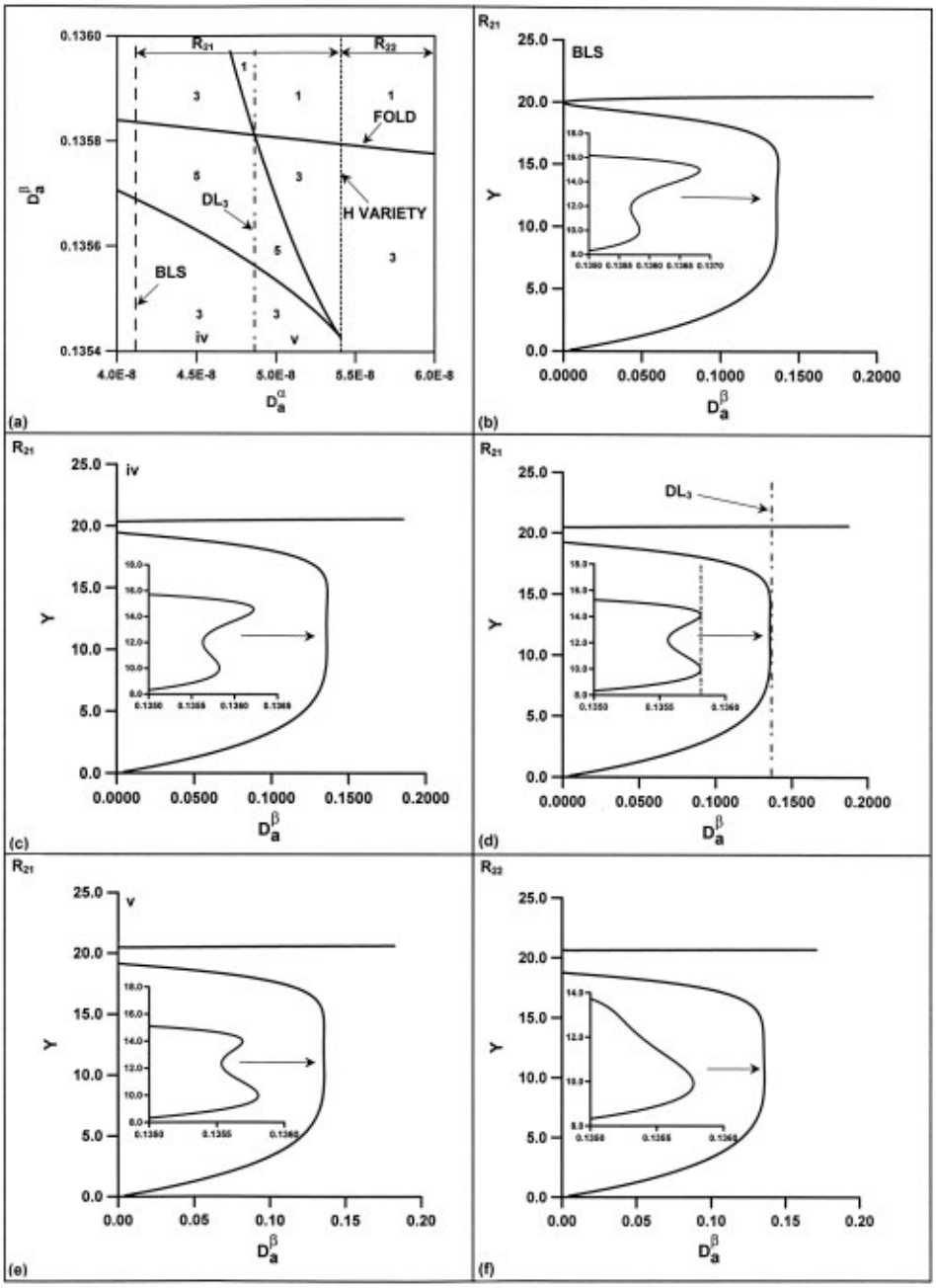

Fig.10. (a) Enlargements of the part of the subregions R_{21} and R_{22} shown in Fig. 5. Representative bifurcation diagrams for the subregions R_{21} and R_{22}. (b) Bifurcation diagram at $D_a^{\alpha} = 4.116965013 \times 10^{-8}$; (c) Bifurcation diagram at $D_a^{\alpha} = 4.5 \times 10^{-8}$; (d) Bifurcation diagram at the double-limit variety DL_3 ($D_a^{\alpha} = 4.865 \times 10^{-8}$); (e) Bifurcation diagram at $D_a^{\alpha} = 5.0 \times 10^{-8}$; (f) Bifurcation diagram at $D_a^{\alpha} = 6.0 \times 10^{-8}$.

Subregion R_{22}

In this subregion one limit point (1 LP) exists as shown in Fig. 10(a) and the representative bifurcation diagram in Fig. 10(f). It is clearly from Fig. 10, that the branches of the solutions intersect with the feasible boundaries at the lower bound $D_a^\beta = 0$.

It is clearly shown in Figures 4-10, that the bifurcation surfaces and the special parameter sets for point 1 at $(\theta = 0.19, \lambda = 21.0)$ is found at small values of D_a^α. Physically, This can be considered as a case for which the reaction in phase β is faster than in phase α or the case of one phase system at saturation. In this case the system is very sensitive to small perturbations (disturbanes) of D_a^α which may affect significantly the steady state operation, control and start-up policy of the reactor.

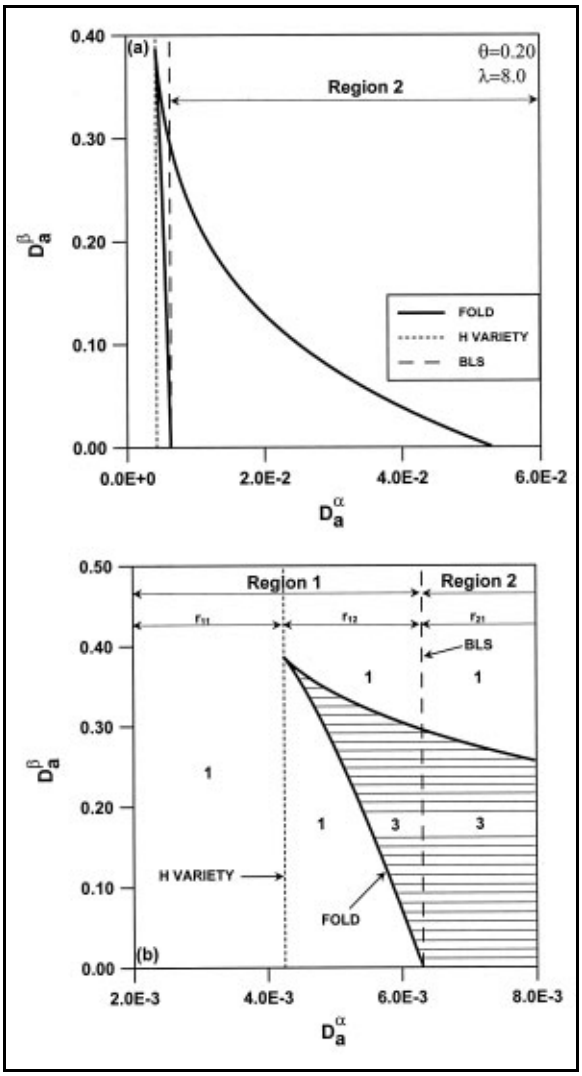

Fig.11. Locus of the fold points in the (D_a^α, D_a^β) plane for the point $(\theta = 0.20, \lambda = 8.0)$ in region 2 shown in Fig.3. (a) Overall diagram; (b) Enlargement of the part of the locus.

The locus of the fold points at point 2 $(\theta = 0.20,\ \lambda = 8.0)$ in region 2 (Fig. 3) is shown in Fig. 11. Since we have a maximum of two limit points, the double-limit variety cannot exist. The boundary limit set (BLS) divides the feasible region into two regions region 1 and 2. The hysteresis variety subdivides region 1 into two subregions r_1 and r_2 depending on the limit points. In the subregion r_1, there are no limit points and therefore a branch of unique

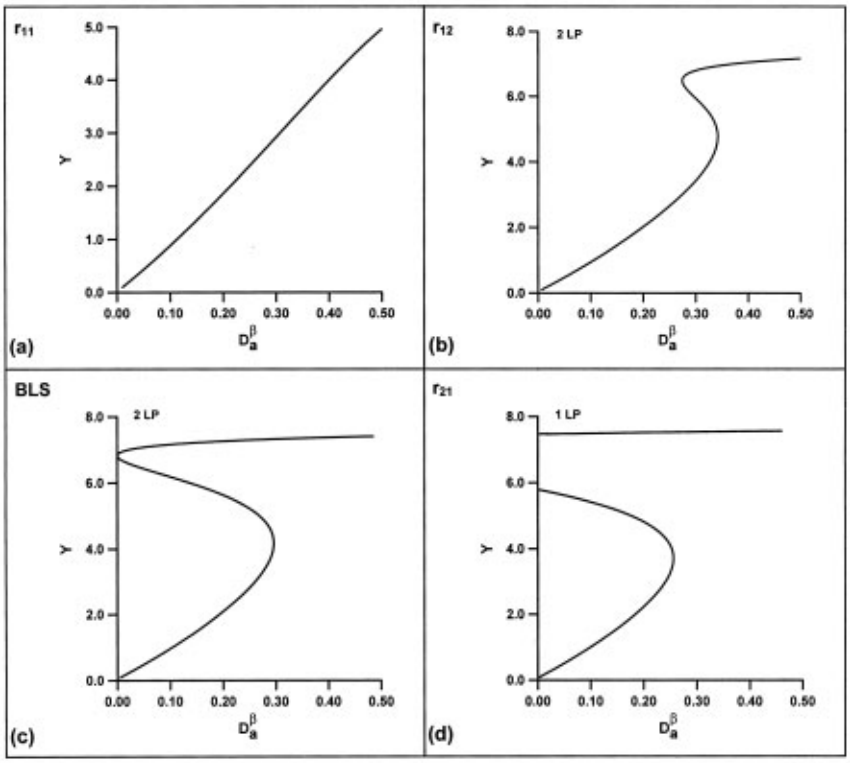

Fig.12. Representative bifurcation diagrams for the subregions r_{11}, r_{12} and r_{21} shown in Fig. 11. (a) Bifurcation diagram in the subregion r_{11} at $D_a^{\alpha} = 2.0 \times 10^{-3}$; (b) Bifurcation diagram in the subregion r_{12} at $D_a^{\alpha} = 5.0 \times 10^{-3}$; (c) Bifurcation diagram in the subregion r_{12} at the boundary limit set ($D_a^{\alpha} = 6.309619213 \times 10^{-3}$); (d) bifurcation diagram in the subregion r_{21} at $D_a^{\alpha} = 8.0 \times 10^{-3}$.

solution exists for all values of D_a^{α} and D_a^{β} as shown by the representative bifurcation diagram in Fig. 12 (a). Two limit points (2 LP) exist in the subregion r_2, result in the possibility of having three steady states as shown in the representative bifurcation diagram presented in Fig. 12 (b). At the boundary limit set (BLS) one limit point exists on the lower bound ($D_a^{\beta} = 0$) as shown in Fig. 12(c). In region 2, one limit point exists and the sequence of the number of solutions is (3,1) when the bifurcation parameter D_a^{β} is changing as shown in Fig. 12(d). This is the situation where a limit point exists outside the feasible region and branches of the solutions intersect with the feasible boundary.

CONCLUSIONS

In this paper an attempt has been made to analyze the two-phase systems in physical equilibrium. This is has been done by using the singularity theory. The theory in a sophisticated manner enables one to divide the global parameter

space into feasible regions of steady state solutions and to predict all the possible multiplicity patterns of these complex systems. One of the main characteristics of this problem is the appearance of two singular points of codimension 4 next to which the steady state manifold can be represented by the butterfly catastrophe. All multiplicity features are confirmed by representative bifurcation diagrams. It appears that the results presented in this study could be useful, for example, in designing experiments for observation of multiple steady state in multiphase systems and in the rational design of these reactors and their control at steady state conditions.

NOTATION

B	dimensionless temperature rise
C_A	overall molar concentration of component A, kmol/m^3
C_P	overall heat capacity, kJ/kmol. K
C_P^i	heat capacity of phase i, kJ/kmol. K
D_a^i	Damköhler number of phase i
E	Activation energy, kJ/kmol
F	total molar flow rate, kmol/s
F^i	molar flow rate of phase i, kmol/s
F_A	total molar flow rate of component A, kmol/s
$-\Delta H_R$	heat of reaction, kJ/kmol
k	reaction rate constant, s^{-1}
k_o	pre-exponential factor, s^{-1}
K_A	Distribution coefficient of componet A
N	total number of moles inside the reactor, kmol
N_A	number of moles of component A inside the reactor, kmol
N^i	number of moles of phase i, kmol
$\mathbf{P}, \mathbf{P}^*$	parameter vectors
q	volumetric flow rate, m^3/s
R	ideal gas constant, kJ/kmol.K
r	ratio of quantity in exit stream to that of reactor contents
T	temperature, K
T_C	cooling coil temperature, K
T^*	dimensionless reference temperature
U	Product of over-all heat transfer coefficient to area of cooling coil, kmol/s.K
V	reactor volume, m^3

v overall molar volume, m^3/kmol

v^i molar volume of phase i, m^3/kmol

x_A^i mole fraction of component A in phase i

Y dimensionless temperature

y^i mole fraction of solvent i

y_A overall mole fraction of component A

Greek Letters

γ^i dimensionless activation energy in phase i

ε ratio of the holding times

θ ratio of activation energies

λ dimensionless heats of reaction

τ total holding time, s

τ^i holding time of phase i, s

ϕ molar ratio of the phases

ψ ratio of volumetric heat capacity of reactor contents to volumetric heat capacity of the feed

Ω^i volume fraction of phase i

Subscripts

C coolant

DL double limit variety

e exit conditions

H hysteresis

L lower bound on variable or parameter

o feed conditions

U upper bound on variable or parameter

Superscripts

α phase α

β phase β

REFERENCES

Abashar, M. E. & Judd, M.R. 1998. Synchronization of chaotic nonlinear oscillators: study of two coupled CSTRs. Chemical Engineering Science **53**: 3741-3750.

Abashar, M. E. & Elnashaie, S. S. E. H. 1997. Complex non-chaotic attractors in fluidized bed catalytic reactors. Transactions of The Institution of Chemical Engineers **75 Part A**: 92-100.

Abashar, M. E., Elnashaie, S. S. E. H. & Hughes, R. 1997. Homoclinicity in the dynamics of forced fluidized bed catalytic reactors. Chaos, Solitons and Fractals **8**: 1655-1684.

Balakotaiah, V. & Luss, D. 1981. Analysis of the multiplicity patterns of a CSTR. Chemical Engineering Communications **13**: 111-132.

Balakotaiah, V. & Luss, D. 1982. Structure of the steady-state solutions of lumped-parameter chemically reacting systems. Chemical Engineering Science **37**: 1611-1623.

Balakotaiah, V. & Luss, D. 1984. Global analysis of the multiplicity features of multi-reaction lumped-parameter systems. Chemical Engineering Science **39**: 865-881.

Doraiswamy, L. K. & Sharma, M. M. 1984. Heterogeneous Reactions: Analysis, Examples, and Reactor Design. Volume 2: Fluid-Fluid-Solid Reactions. John Wiley and Sons, New York, N.Y., U.S.A.

Elnashaie, S. S. E. H. & Abashar, M. E. 1994. Chaotic behavior of periodically forced fluidized bed catalytic reactors with consecutive exothermic chemical reactions. Chemical Engineering Science **49**: 2483-2498.

Gladden, L. F., Mantle, M. D., Sederman, A. J. & Yuen, E. H. L. 2002. Magnetic resonance imaging of single-and two-phase flow in fixed bed reactors. Applied Magnetic Resonance **22**: 201-212.

Golubitsky, M. & Schaeffer, D. 1979. A theory for imperfect bifurcation via sinularity theory. Communications on Pure and Applied Mathematics **32**: 1-77.

Golubitsky, M. & Schaeffer, D. G. 1985. Singularity and Groups in Bifurcation Theory. Springer, New York, N. Y., U.S.A.

Gilmore, R. 1981. Catastrophe Theory for Scientists and Engineers. John Wiley and Sons, New York, N. Y., U.S.A.

Kevrekidis, I. G., Aris, R. & Schmidt, L. D. 1986. The stirred tank forced. Chemical Engineering Science **41**:1549-1560.

Kubicek, M. & Marek, M. 1983. Computational Methods in Bifurcation Theory and Dissipative Structures. Springer-Verlag, New York, N.Y., U.S.A.

Planeaux, J. B. & Jensen, K. F. 1986. Bifurcation phenomena in CSTR dynamics: A system with extraneous thermal capacitance. Chemical Engineering Science **41**: 1497-1523.

Pais, F. I. C. C. & Portugal, A. A. T. G. 1996. Steady state behaviour of isothermal two-phase continuous stirred tank reactors for extreme solids concentrations. Chemical Engineering Science **51**: 321-323.

Schmitz, R. A. & Amundson, N. R. 1963a. An analysis of chemical reactor stability and control-Va. Two-phase systems in physical equilibrium-1. Chemical Engineering Science **18**: 265-289.

Schmitz, R. A. & Amundson, N. R. 1963b. An analysis of chemical reactor stability and control-Vb. Two-phase systems in physical equilibrium-2. Chemical Engineering Science **18**: 391-414.

Trambouz, P. 1961. Reactor design relations for two-phase liquid-liquid processes. Chemical Engineering Science **14**: 161-175.

Uppal, A., Ray, W. H. & Poore, A. B. 1974. On the dynamic behavior of continuous stirred tank reactors. Chemical Engineering Science **29**: 967-985.

Van Heerden, C. 1953. Autothermic processes. Industrial & Engineering Chemistry **45**:1242-1247.

Received *: 22-3-2003*
Revised *: 9-12-2003*
Accepted *: 21-12-2003*

تحليل التشعبات العام لأنظمة طورين في المفاعلات دائمة الخلط

محمد البشير الأمين أبشر

قسم الهندسة الكيميائية- كلية الهندسة- جامعة الملك سعود
ص. ب. 800- الرياض 11421- المملكة العربية السعودية

خلاصة

لقد درست مسألة طورين في المفاعلات دائمة الخلط من منظور التحليل العام للتشعبات في حالة الاستقرار. ويعتمد هذا البحث علي نظرية الفردية التي تقسم فضاء المتغيرات إلى مناطق تحتوي علي حلول ورسومات تشعبات متعددة. ولقد وجد أن هذأ النهج المتميز يعطي مفاهيم يصعب الحصول عليها بواسطة الطرق العددية ودراسة تغير المتغيرات. ولقد كشفت هذه الدراسة جزء كبير من خواص حالات الاتزان لهذه النظم المعقدة. وكذلك كشفت هذه المسألة خاصتين هامتين هما، وجود نقطتين فرديتين (فراشة) عند أعلي بعد في المناطق ذات الجدوى. ولقد وجد أن هنالك مناطق تحتوي علي خمسة حالات اتزان ورسومات تشعبات متقطعة الفروع.